ABSTRACT BOOK

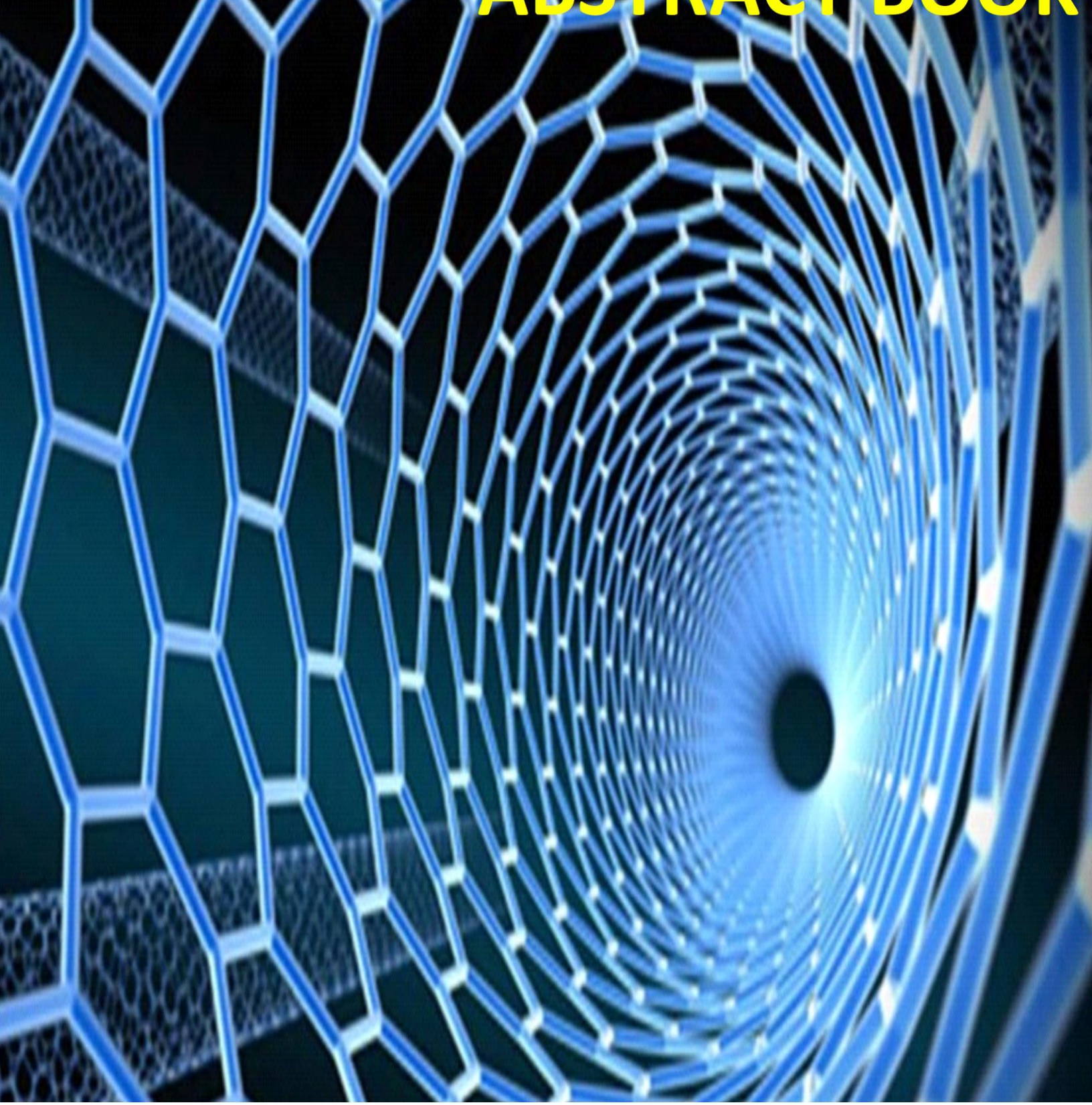

Advances in Functional Materials

InterContinental Nanjing, China

Aug 27-Aug 30, 2018

Forced Electrical Stress based Direct Current Generator Via Triboelectric Effect 35

Efficiency Enhancement of Dye Sensitized Solar Cells with Metal-ion-adsorbed ZnO Nonorods 36

Site-Specific Delivery of Hybrid Upconversion Nanoparticles for Photo-Activated Multimodal Therapies of Glioblastoma 37

Antiferromagnetic ordering of lithium deintercalated Fe1-xZnxPO4 by Mössbauer spectroscopy 38

Tunable Arsenene bandgap in Arsenene-Graphene heterostructures 39

Crystal structure and magnetic properties of fluorophosphates Na2Fe0.9Mn0.1PO4 F cathode material 40

High-Performance Planar Crosslinked Polyaniline Based Microsupercapacitors 41

Structural color filters with improved color purity by suppressing higher-order resonances 42

Enhanced Magnetoresistance Induced by Coherent Magnon Current in Magnon Valve... 42

Fabrication of Superhydrophobic Surfaces Using Electrohydrodynamic Lithography 43

Silk Film supported reduced Graphene Oxide Field Effect Transistor 44

The Effect of Talc Concentration on the Peeling Characteristics of UV-curable Acrylic Coating Agent 45

Growth of nb dopped MoS2 using RF sputtering and its physical properties 46

Supercapcitor performance of carbon nanofiber electrodes derived from 6FDA-based polyimides 47

High sensitive piezoelectric acoustic sensor based on two dimensional MoS2 48

Growth of Large-Area AB-Stacked Bilayer Graphene on h-BN/Pt Foils by Chemical Vapor Deposition 49

Three-dimensional perovskite-type oxide nano-fiber webs for soot oxidation 50

High photoluminescence properties of transparent nanofiber using C-dots 51

Study on the force transfer by external force to a molecular level using spiropyran molecular sensor covalently linked polyurethane 52

Dopant-free hole transport meaterials for p-i-n planar perovskite solar cells paasivating defect site at the interface 53

p18-4-Conjugated Polymeric Nanohybrids for Enhanced Breast Cancer Targeting in Photodynamic Therapy 54

Thermal and Mechanical Properties of Porous Polymeric Composites Prepared by UV-Curing Process 55

Advances in magnetic biochar adsorptive characteristics enhancements: Role of production route and in/ex-situ magnetic-field effect 56

Electrospun PAN/PAA nanocomposite with high transparency and superfine fibrils 57

Antiferromagnetic ordering of lithium deintercalated Fe1-xZnxPO4 by Mössbauer spectroscopy

Hyunkyung Choi, Chul Sung Kim

Kookmin University, Korea, Republic of (South Korea); newton@kookmin.ac.kr

The structural and magnetic phase transitions in lithium deintercalated Fe1-xZnxPO4 (x=0.0, and 0.02) were investigated by x-ray diffraction, vibrating sample magnetometer, and Mössbauer spectroscopy. The crystalline structure of the Fe1-xZnxPO4 were determined to be orthorhombic with space group Pnma. The Fe1-xZnxPO4 compared to LiFe1-xZnxPO4 had enhanced lattice distortions along the c-axis because the unit cell volume decreased due lithium deintercalaction. The temperature dependence of magnetic susceptibility of Fe1-xZnxPO4 show antiferromagnetic behaviors. The Néel temperature (TN) decreased from 114 K for FePO4 to 82 K for Fe0.8Zn0.2PO4. Also, temperature dependent Mössbauer spectra of Fe1-xZnxPO4 below TN were fitted with eight-lines Lorentzian (the relatively small lines). The room temperature Mössbauer spectrum shows one-doublet with the measured values of electric quadrupole splitting ΔEQ = 1.51 mm/s, and isomer shift δ = 0.31 mm/s for x=0; ΔEQ= 1.38 mm/s, and δ = 0.31 mm/s for x=0.2 indicating ferric (Fe3+) ions. These values decreased with increasing Zn content due to decreasing number of interactions between Fe ions. The magnetic hyperfine field (Hhf), polar angle (θ), azimuthal angle (φ), asymmetric parameter (η), ratio of electric quadrupole interaction to magnetic dipole interaction (R) values of the Fe0.8Zn0.2PO4 at 4.2 K were determined to be Hhf = 491.43 kOe, θ = 66, φ = 49, η = 0.8, and R = 0.5. We conclude that the different value of hyperfine field and magnetic susceptibility, indicating that the superexchange interaction via Fe-O-Fe link is stronger than that for Fe-O-Zn link.